Bose-Einstein condensates and the spectrum of excitations in a two-dimensional channel

I. V. Shunyaev,[1,*] A. A. Elistratov,[2] and Yu. E. Lozovik[3,4]
[1]*Moscow State Pedagogical University, 119571 Moscow, Russia*
[2]*N. L. Dukhov All-Russia Research Institute of Automatics, Moscow, Russia*
[3]*Institute for Spectroscopy RAS, 142190 Troitsk, Moscow, Russia*
[4]*Moscow Institute of Physics and Technology (State University), 141700 Dolgoprudny, Moscow region, Russia*
(Received 13 June 2016; published 28 November 2016)

The transverse spatial distribution of weakly interacting Bose gas in a narrow channel is found. The corresponding analytical solution of the Gross-Pitaevskii equation has the form of a cnoidal wave. The possible physical realization of the model is a system of cold atoms or quasiparticles, e.g., excitons, cavity photons, exciton polaritons. The obtained formula is used for the numerical calculation of the spectrum of excitations and the critical velocity of the condensate. These numerical results do not coincide with the Bogoliubov spectrum, and we show that the strongly inhomogeneous condensate density leads to larger values of the critical velocity. We also make numerical estimation of the critical velocity for various types of considered particles or quasiparticles.

DOI: 10.1103/PhysRevA.94.053625

I. INTRODUCTION

Bose condensation of atoms and quasiparticles, such as excitons [1,2], cavity photons [3,4], and exciton polaritons [5–10], is one of the most popular objects of study in modern physics due to the fundamental nature of the phenomenon and great opportunities for various applications of it [11–20]. The Bose condensation of quasiparticles (excitons, cavity photons, exciton polaritons) was experimentally obtained in low-dimensional systems. The evidence for condensation of excitons was reported in two-dimensional structure with coupled quantum wells [21] and in a single quantum well [22]. Several works were dedicated to the superfluid flowing of Bose condensate along low-dimensional guiding structures and similar devices [23–29]. A device, which is analogous to a transistor, but based on flowing of the polariton condensate, was suggested [30]. It was suggested to use the flowing polariton condensate in a wide Y-shaped channel as an optical switch [31]. The two-fluid polariton switch was investigated in [32]. A polariton quantum gyroscope, based on the formation of vortex pairs in the polariton condensate flowing in a ring-shaped channel, was proposed in [33].

The majority of works use the mean-field approximation, describing the possible states and behavior of the Bose-Einstein condensate. In this work we present the exact analytical solution, describing the ground state of the Bose condensation in the two-dimensional guiding structure having the form of a long, narrow channel. The structure under consideration is close to the cigar-shaped one-dimensional traps experimentally realized by Görlitz *et al.* [34] for the condensates of cold atoms, though in our work the cylindrical geometry of the trap is replaced by a rectangular one. The trap of such a geometry (three-dimensional optical box) was experimentally realized for atoms [35]. The solution, which we found, stays valid at an arbitrary value of the interparticle interaction parameter and width of the channel. The inhomogeneity of the spatial distribution of the condensate density in the trap causes a dramatic rise of the critical velocity of the condensate in comparison with homogeneous distribution of the condensate. Our results are universal for all types of condensed particles and quasiparticles. We have chosen the gas of rubidium atoms as an object of investigation for numerical calculations, though the considered system can be realized in other atomic gases, excitons, and exciton polaritons. The atomic gas is chosen due to the fact that a lot of experimental works devoted to the measurement of the critical velocity of the condensate were realized in the condensates of atoms (for example, in optical lattices of various dimensionality).

II. TRANSVERSE DENSITY SPATIAL DISTRIBUTION OF THE CONDENSATE IN TWO-DIMENSIONAL CHANNEL

To solve the problem we first obtain the density distribution function $n(x,t)$ of the condensate. Here we suppose that the density varies along x, which we direct across the channel, and is uniform along y, directed along the channel. The density distribution can be derived from the Gross-Pitaevskii equation:

$$\left(-\frac{\hbar^2}{2m}\triangle + g\, n(x,t)\right)\Psi(x,t) = i\hbar\frac{\partial}{\partial t}\Psi(x,t), \qquad (1)$$

where m is the effective mass of the particles, g is the interparticle interaction parameter, $\Psi(x,t) = \sqrt{n(x,t)}\exp[iS(x,t)]$ is the wave function of the condensate, and $S(x,t)$ is its phase. We have the boundary conditions $n(0) = n(L) = 0$, where L is the width of the channel. Substituting the formula for wave function of the condensate into (1), we get the set of equations, which reads

$$\frac{\partial n}{\partial t} + \frac{\hbar}{m}\nabla(n\nabla S) = 0$$
$$\hbar\frac{\partial S}{\partial t} + \frac{\hbar^2}{2m}(\nabla S)^2 + gn - \frac{\hbar^2}{2m\sqrt{n}}\nabla^2\sqrt{n} = 0. \qquad (2)$$

First, we consider the stationary solution of (2), so we suppose $S(x)$ to be constant and introduce $\frac{\partial S}{\partial t} = -\frac{\mu}{\hbar}$, where μ is the chemical potential. Then from (2) we get the equation

$$-\mu + gn + \frac{\hbar^2}{8mn^2}\left(\frac{\partial n}{\partial x}\right)^2 - \frac{\hbar^2}{4mn}\frac{\partial^2 n}{\partial x^2} = 0. \qquad (3)$$

*walmail89@mail.ru

Substituting $\frac{\partial n}{\partial x} = p$ in (3), we get

$$-\mu + gn + \frac{\hbar^2}{8mn^2}p^2 - \frac{\hbar^2}{4mn}\frac{\partial p}{\partial x} = 0. \quad (4)$$

Equation (4) does not contain the coordinate explicitly, so the further algorithm of actions is standard: substituting $Z = \frac{p^2}{2}$, we transform Eq. (4) into first-order a differential equation:

$$\frac{dZ}{dn} = \frac{4mgn^2}{\hbar^2} + \frac{Z}{n} - \frac{4mn\mu}{\hbar^2}. \quad (5)$$

Solving Eq. (5) by the method of variation of constants, we get Z:

$$Z = n\left(\frac{2mgn^2}{\hbar^2} - \frac{4mn\mu}{\hbar^2} + C\right). \quad (6)$$

Here C is the integrating constant. Making a transformation from (Z,n) to (n,x) we obtain the following differential equation:

$$dx = \frac{dn}{\sqrt{2n\left(\frac{2mgn^2}{\hbar^2} - \frac{4mn\mu}{\hbar^2} + C\right)}}. \quad (7)$$

Factoring the denominator in (7) we get an equation that reads

$$\frac{\sqrt{2mg}}{\hbar}dx = \frac{dn}{\sqrt{2n(n-\gamma^-)(n-\gamma^+)}}, \quad (8)$$

where

$$\gamma^{\pm} = \frac{\mu}{g} \pm \sqrt{\left(\frac{\mu}{g}\right)^2 - \left(\frac{c}{g}\right)^2}, \quad c^2 = \frac{\hbar^2 gC}{2m}. \quad (9)$$

In order to integrate (8) we use the substitution $n = \gamma^- \sin^2(\varphi)$ and get the elliptic integral of the first kind:

$$\begin{aligned}\frac{\sqrt{2mg}}{\hbar}x &= \int_0^{n'} \frac{dn}{\sqrt{2n(n-\gamma^-)(n-\gamma^+)}} \\ &= \sqrt{\frac{2}{\gamma^+}}\int_0^{\varphi} \frac{d\varphi}{\sqrt{1-\frac{\gamma^-}{\gamma^+}\sin^2(\varphi)}} \\ &= \sqrt{\frac{2}{\gamma^+}}F\left(\arcsin\left(\frac{n}{\gamma^-}\right), \sqrt{\frac{\gamma^-}{\gamma^+}}\right). \end{aligned} \quad (10)$$

The condensate density n can be found from Eq. (10) with the help of Jacobi elliptic function $\mathrm{sn}(u,k)$, where u is the variable of the elliptic function and k is the elliptic modulus:

$$n(x) = \gamma^- \mathrm{sn}^2\left(\sqrt{\frac{\gamma^+ mg}{\hbar^2}}x, \sqrt{\frac{\gamma^-}{\gamma^+}}\right), \quad (11)$$

where $\gamma^- > 0$ and $\gamma^+ > 0$. This solution can be called a stationary cnoidal wave. It is governed by three parameters: γ^-, γ^+, and the interaction parameter g. The parameter γ^- obviously is an amplitude of the density spatial distribution. γ^+ cannot be physically interpreted, but all three parameters $\gamma^{\pm}$ and g determine the period of the condensate wave function. The values of the parameters can be determined via the boundary conditions and the requirement of the density distribution being normalized to the full number of particles in the condensate.

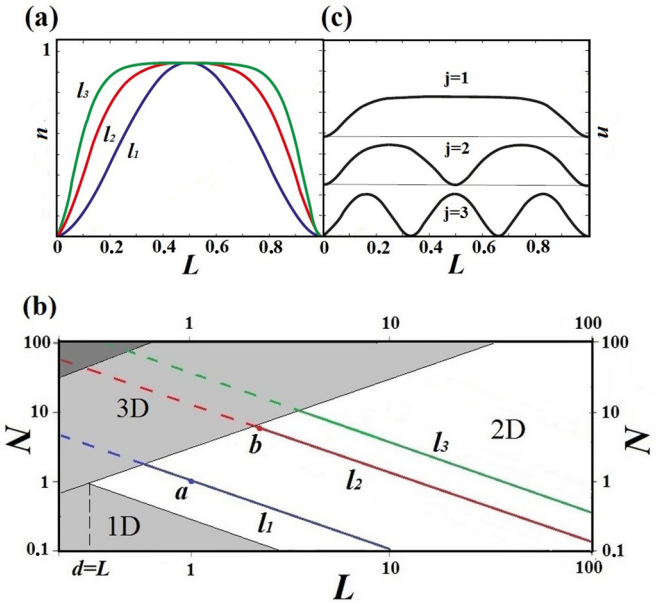

FIG. 1. (a) The spatial distribution of normalized density of the condensate in the channel for $l = L/\xi = \text{const}$. (b) The relationship between the number of particles N per μm and the width of the channel L for several values of $l = L/\xi$, corresponding to the profiles of the density above. The graphs are provided for the atoms of rubidium at $g = 1{,}5$ peV $\times\ \mu\text{m}^2$. Each line corresponds to the constant values of l and constant density profile. Two dots on the lines l_1 and l_2 in the graph (b) show the states used for further numerical calculations. Grey regions show 3D and 1D regimes at thickness of the trap $d = 0{,}3$ μm. The dark grey region in the upper left corner corresponds to dense Bose gas, where $Na^3/(dL) > 1$. The scattering length, used for the calculations, is approximately 66 nm. (c) Normalized density profiles for $j = 1$, $j = 2$, and $j = 3$ at one and the same value of the chemical potential.

It follows from the boundary and the normalization conditions that the solution must satisfy a set of equations

$$\begin{aligned}(\gamma^- + \gamma^+)\xi^2 &= \frac{2}{\Gamma} \\ N &= \int_0^{L/\xi} \gamma^- \xi \,\mathrm{sn}^2\left(\sqrt{\frac{\gamma^+\Gamma\xi^2}{2}}\eta, \sqrt{\frac{\gamma^-}{\gamma^+}}\right)d\eta \\ L &= 2j\sqrt{\frac{2}{\gamma^+\Gamma}}K\left(\sqrt{\frac{\gamma^-}{\gamma^+}}\right). \end{aligned} \quad (12)$$

Here N is the number of particles per unit of length in the condensate, $K(k)$ is the complete elliptic integral of the first kind, $\xi = \frac{\hbar}{\sqrt{2m\mu}}$ is the spatial scale, which coincides with the healing length in a wide channel, where the spatial distribution of the condensate is nearly homogeneous. $\Gamma = \frac{2mg}{\hbar^2}, \eta = x/\xi, j = 1,2,3\ldots$ is the number of solution and $j = 1$ corresponds to the ground state of the condensate. N, L, and Γ are related to the γ^-, γ^+, and g here.

A number of solutions may exist in the channel. They differ from each other in their energy and their density profile. The density spatial distribution for $j = 1$, $j = 2$, and $j = 3$ is shown in Fig. 1(c).

The system possesses an interesting inner symmetry, which can be seen from the set (12): at different values of the chemical potential and the width of the channel the density distribution may have one and the same profile, if L/ξ stays constant and the value of Γ is not changed (it can be tuned by Feshbach resonance). As it is shown in Fig. 1, in an $N-L$ diagram these constant profiles correspond to hyperbolas. In Fig. 1(b) there are several solid lines, depicting these hyperbolas in logarithmic scale at fixed value of Γ for several values of L/ξ. Corresponding density profiles are provided for each line in Fig. 1(a).

Choosing L as a spatial scale, we are able to rewrite the set (12) in the following way:

$$\begin{aligned}\gamma^{-'}+\gamma^{+'} &= \frac{2\mu}{\Gamma}\\ N' &= \int_0^1 \gamma^{-'}\mathrm{sn}^2\left(\sqrt{\frac{\gamma^{+'}m\Gamma}{\hbar^2}}\eta,\sqrt{\frac{\gamma^{-'}}{\gamma^{+'}}}\right)d\eta\\ 1 &= 2j\sqrt{\frac{\hbar^2}{\gamma^{+'}m\Gamma}}K\left(\sqrt{\frac{\gamma^{-'}}{\gamma^{+'}}}\right),\end{aligned} \tag{13}$$

where $\gamma^{\pm'}=\gamma^{\pm}L^2$, $\Gamma=g/L^2$, $\eta=x/L$, and $N'=NL$. If g is constant, the only controlling parameter, which determines the form of the density profile, is N', as then parameters $\gamma^{\pm'}$ included into the density (11) can be easily calculated. It means that in fact at constant g the density profile is determined by the relation $N'=N\times L=\mathrm{const}$.

From the condition $\xi > d$, where d is the thickness of the trap for atoms, or of the quantum well for quasiparticles, we obtain the condition of low-dimensionality for our system: $N_{2D} < \frac{\hbar^2 L}{2mgd^2}$. Reducing the width of the channel L we are able to proceed into the region of $N-L$ diagram, where the condensate demonstrates the properties of one-dimensional Bose gas. The crossover happens, if $\xi > L$. The estimation gives the following condition of one-dimensionality: $N_{1D} < \frac{\hbar^2}{2mgL}$. These inequalities define the borders of the region of our interest, the numerical estimations of these borders are shown in Fig. 1(b), where the regions of the three-dimensional (3D) and 1D cases are grey. The borders of 3D and 1D regions cross at $L=d$. We also take into account that the mean-field approximation is correct only if the following inequality is satisfied: $\frac{N}{dL}a^3 < 1$ (here a is the scattering length), which means that the gas is not dense. The region of dense Bose gas is shown in Fig. 1(b) in dark grey color. The condition is written for 3D gas, as numerical calculation shows that in the system under consideration this condition may be not satisfied only for 3D Bose gas.

We avoid the consideration of the region of extremely low density, as in this limit condensate transits into an asymptotic regime, analogous to the Tonks-Girardeau regime in one dimension, where interaction parameter g no longer depends on the scattering length, but depends on the density [36–38]. The criterion for this transition is given by the inequality [17]

$$|\ln(nd^2)| > \sqrt{2\pi d/a}. \tag{14}$$

According to (14) the critical density value for this transition is determined primarily by the ratio of the axial thickness of the trap d and the scattering length a. In the regime the correlation between N,L,g and the profile of the condensate density is much more complicated and such value of the average density (less than $10^{-4}\ \mu\mathrm{m}^{-2}$ for typical experimental values of a for the atoms of rubidium) is of little practical use. In Bose gas of excitons this regime may occur at larger values of the density due to the larger typical values of the scattering length for excitons than for atoms, so this type of particle should be treated more carefully. But one should bear in mind that the scattering length can be tuned to the lower values by Feshbach resonance making Fig. 1(b) also correct for the excitons.

Now we analyze several extreme cases: the ideal Bose gas, dilute weakly interacting Bose gas, and dense weakly interacting Bose gas.

In the limit of ideal gas $g \to 0$ and $\frac{\gamma^-}{\gamma^+} \to 0$. Then from the second equation of (12) we have $\mu=\mu_0+\delta\mu$, where $\mu_0=\frac{\pi^2 j^2\hbar^2}{2mL^2}$. The expression for $\delta\mu$ provides us with the correlation between the number of particles and the chemical potential:

$$\delta\mu = \sqrt{2}gN/L. \tag{15}$$

The density is

$$n(x)=\frac{2N}{L}\mathrm{sn}^2\left(\frac{\pi j}{L}x,0\right)=\frac{2N}{L}\sin^2\left(\frac{\pi j}{L}x\right). \tag{16}$$

Equation (1) is formally transformed into the Schrödinger equation for one particle, while all the possible values of the chemical potential μ_0 are given by the spectrum of one-particle states. The energy of the condensate is given by the formula

$$E=\int_0^L\left[\frac{\hbar^2}{8mn}\left(\frac{dn}{dx}\right)^2+\frac{g}{2}n^2\right]dx. \tag{17}$$

Integrating (17), we get

$$E=N\mu_0. \tag{18}$$

In this limit solution (11) reminds one of the solution for a square of the wave function of a particle in a potential box, and the energy of the condensate equals the sum of energies of separate particles μ_0. The healing length is then transformed into $\xi_0=\frac{L}{j\pi}$ and for $j=1$ associated with the half of the wavelength $\lambda/2=\pi\xi_0$.

It is also useful to find an approximate explicit relation between $\gamma^{\pm}$ parameters and the chemical potential. In the limit of a small value of g we have

$$\gamma^- = 4\sqrt{\left(\frac{\mu_0}{g}+\frac{\sqrt{2}N_0}{L}\right)\left[4\left(\frac{\mu_0}{g}+\frac{\sqrt{2}N_0}{L}\right)+\frac{2N_0}{L}\right]} - \frac{8\mu_0}{g}-\frac{N_0}{\sqrt{2}L}, \tag{19}$$

where N_0 is the number of weakly interacting particles. This expression turns into $\frac{2N_0}{L}$ at $g=0$ for the ideal gas. γ^+ is equal to $\frac{2\mu}{g}-\gamma^-$.

In the case of dilute Bose gas ($N/L \to 0$) we have the same expression for the chemical potential, but the formula for γ^- is different:

$$\gamma^- = \frac{2N}{L}+\frac{25g}{28\mu_0}\frac{N^2}{L^2}. \tag{20}$$

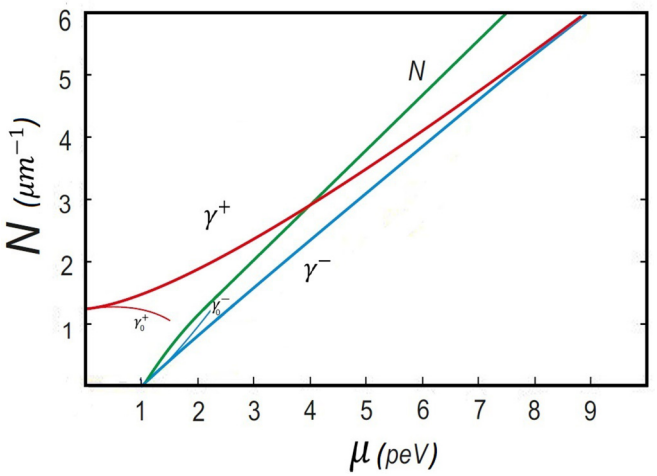

FIG. 2. The relationship between the key parameters of the system [$\gamma^{\pm}$ (red and blue lines), number of particles per unit of length N (green line)] and the chemical potential (expressed in peV) at fixed $L = 2\mu$m and $g = 1.5$ peV $\times\ \mu$m^2 for atoms of rubidium. The values of γ^+ (red line) and γ^- (blue line) differ at small values of μ and approach each other, as μ grows. Short thin curves depict the approximate values of γ_0^+ and γ_0^-, given by (20).

The numerical relation between γ^-, γ^+, and μ is given in Fig. 2, as well as the approximate values of these parameters, calculated via the expressions provided above for the dilute Bose gas at constant value of the interaction parameter. As we can see, these expressions are correct only in a small range of values of the chemical potential. In the limit of dense Bose gas $N \to \infty$ we have

$$N = L\frac{\mu}{g} - \frac{2j\hbar}{g}\sqrt{\frac{\mu}{m}} \times \tanh\left(\sqrt{\frac{\mu m}{\hbar^2}}L\right). \tag{21}$$

We see that all of the states of condensate have one and the same limit for chemical potential $\mu = gn$, corresponding to the local Thomas-Fermi density.

In the approximation of large values of the chemical potential the following relation is found:

$$\gamma^{\pm} = \frac{\mu}{g}\left(1 \pm 8 \times \exp\left[-\frac{L\sqrt{\mu m}}{j\hbar}\right]\right). \tag{22}$$

If the chemical potential is large enough, the exponential term quickly decreases, and the relation turns out to be also linear.

To obtain the formula for the energy of the dense condensate in the channel we integrate (17) after several algebraic transformations and series expansion of the first term of the integral near the value of the modulus of the elliptic function $\sqrt{\gamma^-/\gamma^+} = 1$. We also remark that the partial derivative of the result $\mu = \partial E/\partial N$ gives the first equation of the set (12) in dimensional form. We substituted into the result of integrating (21) and (22) and used the approximation of wide channel $L/\xi \to \infty$, expanding the obtained expression into the series. The result of these transformations for the ground state of the condensate is

$$E = \frac{4}{3}\hbar n\sqrt{\frac{gn}{m}} + \frac{gn^2}{2}L - 2\sqrt{2}gn^2\xi, \tag{23}$$

where the first term is the energy of motionless soliton, the second term is the energy of the uniform Bose condensate, and the last term is the correction proportional to the healing length ξ and the square of the density n. This correction reduces the region of the uniform Bose condensate from the width of the channel L by the size of the double healing length.

III. SPECTRUM OF EXCITATIONS AND THE CRITICAL VELOCITY OF THE CONDENSATE

Now we can use the obtained $n(x)$ to find the spectrum of the excitations ε via solution of Bogoliubov–de Gennes equations:

$$\begin{aligned}\left(-\frac{\hbar^2}{2m}\triangle - \mu + 2gn(x)\right)u(\mathbf{r}) + gn(x)v(\mathbf{r}) &= \varepsilon u(\mathbf{r})\\ \left(-\frac{\hbar^2}{2m}\triangle - \mu + 2gn(x)\right)v(\mathbf{r}) + gn(x)u(\mathbf{r}) &= -\varepsilon v(\mathbf{r}),\end{aligned} \tag{24}$$

where $r^2 = x^2 + y^2$, and $u(\mathbf{r})$ and $v(\mathbf{r})$ are Bogoliubov coefficients. Here we see that condensate $n(x)$ plays a role of an effective external potential for functions $u(\mathbf{r})$ and $v(\mathbf{r})$. The set (24) was solved numerically; the results for several combinations of the controlling parameters N and L are shown in Fig. 3. The results in the figure are given in dimensionless units with energy scale of 10^{-12} eV and 10^{-6} m as spatial scale. These numerical results are compared to the spectrum, calculated via the Bogoliubov formula:

$$\varepsilon = \sqrt{\frac{\hbar^2k^2}{2m}\left(\frac{\hbar^2k^2}{2m} + 2gn\right)}. \tag{25}$$

To calculate spectrum via (25) we use the average density $n = N/L$. The result of such "formal" use of the formula (25) is a rude effect of a gap in the spectrum of excitations. The resulting spectra are shown in Fig. 3 by dashed lines. We see that in the narrow system such straightforward use of the formula (25) gives wrong result, though in a wide channel the result is correct and the spectrum is gapless. The valid spectrum, shown by the solid lines, has no gap and has phononic shape in the region of small values of the longitudinal momentum. The difference between the numerical results and the results obtained via (25) is obviously explained by the strong inhomogeneity of the condensate density in the narrow channel, as formula (25) is correct only for the uniform condensate. The dashed and solid lines, as k_y (longitudinal momentum) increase, approach each other and coincide at large values of the longitudinal momentum, where the density-dependent member does not play a crucial role. At low values of N the spectrum is parabolic. As the number of particles and density are increased, the spectrum becomes more linear in the region of the small longitudinal momentum. The change of the values of the interaction parameter g causes the same effect.

The spectra of excitations for the excited states of the condensate are always complex with positive imaginary part, the examples of which are shown in the inset of Fig. 3. Here, the diagram of Im(ε) looks like a bell, the height and width

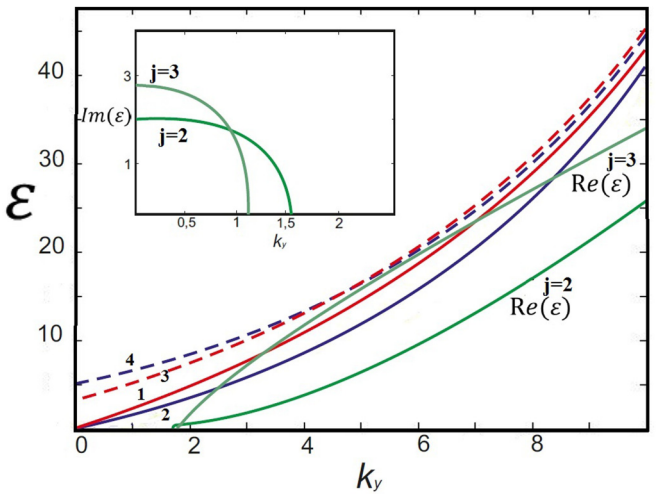

FIG. 3. Examples of the spectrum of excitations for the states of the rubidium atoms, shown by the dots in Fig. 1(b) at $g = 1.5$ peV $\times$ μm^2. The red line 1 shows the numerical results for the spectrum at $N = 7$ μm^{-1} and $L = 2$ μm, the dark blue line 2 shows $N = 1$ μm^{-1} and $L = 1$ μm. The dashed red line 3 and dashed dark blue line 4 show the spectrum, calculated via the Bogoliubov formula, which gives spectrum with a gap in the narrow channel. The spectra do not coincide due to the heterogeneity of the condensate density. The green lines $j = 2$ and $j = 3$ in the main diagram show the real parts of the energy of excitations for the cases of the excited states of the condensate with corresponding j. The numerical values used in calculations are $L = 1$ and $N = 1$ for the excited state of the condensate $j = 2$; $L = 2$ and $N = 7$ for the excited state of the condensate with $j = 3$. The inset in the upper left corner shows the corresponding imaginary parts, indicating the existence of an instability for the excited states of the condensate. The energy ε and the longitudinal momentum k_y are given in dimensionless units.

of which grow as N and L are reduced. They are also larger for the excited states of higher order ($j = 3$,4,5 and so on) even at the same values of the controlling parameters. The corresponding real parts Re(ε) are also provided in Fig. 3. It shows that all the states except the ground state are unstable.

The obtained spectra allow us to calculate the critical velocity using Landau criteria. The results for the critical velocity are shown in Fig. 4 by solid lines. These results are compared to the sound velocity $c_s = \sqrt{gn/m}$ of a uniform condensate, shown in Fig. 4 by dashed lines, as for a linear spectrum the critical velocity and the sound velocity coincide. Obviously, the critical velocity in our nonuniform system increases faster than the sound velocity of a uniform Bose gas, as we reduce the width of the channel due to the heterogeneity of the spatial distribution of the density. In a wide channel these parameters coincide, but the inhomogeneity leads to the sharp increase of the critical velocity at small values of L, which shows the advantage of 1- or 2-μm-wide channels as guiding structures for the condensate. According to our results, at such width of a channel it is possible to obtain atomic condensates with critical velocity up to 8–12 mm/s, which is several times larger than the critical velocity of 2D rubidium condensate (0.5–1 mm/s in [39]), or rubidium condensate in 1D optical lattice (up to 1.5 mm/s in [40]).

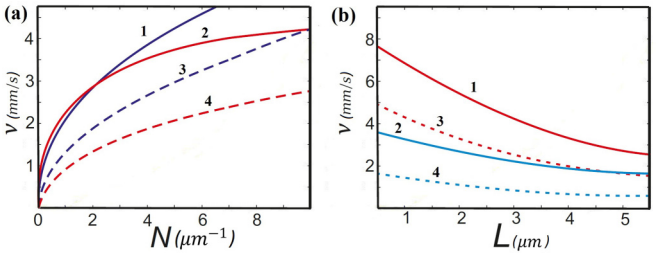

FIG. 4. (a) The relation between the critical velocity of the condensate of rubidium atoms and the number of particles per unit of length at constant width of the channel, expressed in μm. Here $L = 2$ for the solid red line 2 and dashed red line 4 and $L = 1$ for the solid dark blue line 1 and dashed dark blue line 3. (b) The relation between the critical velocity of the condensate of rubidium atoms and the width of the channel L at constant number of particles per unit of length N, given in μm^{-1}. Here $N = 1$ for the solid blue line 2 and dashed blue line 4 and $N = 7$ for the solid red line 1 and dashed red line 3. The valid dependence is given by solid lines, and the one calculated via the formula for the sound velocity is given by the dashed lines. We see that at low values of L and at large values of N the critical velocity increases faster than the sound velocity of a uniform gas for the same values of the average density n.

We have also made an estimation of the critical velocity for excitons and exciton polaritons for the same values of L and N, shown by points (a) and (b) in Fig. 1(b). For numerical estimation we have used $g = 6 \times 10^{-6}$ eV $\times$ μm^2, which approximately corresponds to the typical experimental results for excitons and polaritons [41]. The value of critical velocity for excitons in the channel for $L = 1$ μm and $N = 1$ μm^{-1} is $v = 3.64 \times 10^3$ m/s and 5.46×10^3 m/s at $L = 2$ μm and $N = 7$ μm^{-1}. These values approximately correspond to the value of the sound velocity of excitons in [25]. The value of the critical velocity of polaritons at the same parameters varies from 1.3 to 1.4×10^7 m/s vs 1.8×10^6 m/s in [31] or approximately 4.5×10^6 m/s in [26].

IV. CONCLUSIONS

We have obtained the exact analytical expression for the spatial density distribution of the condensate in a two-dimensional narrow channel. In fact, the expression (11) and set of equations (12) are valid not only for the ground state of the condensate, but correctly describe the excited states, characterized by the existence of an arbitrary number of solitons in the density profile, as well. We also demonstrate that these excited states are not stable. The spectrum of excitations and the critical velocity have been calculated. We have demonstrated that the results do not coincide with the Bogoliubov spectrum. The solution which we provided here can be applied to any Bose condensate, including atomic condensates, condensates of excitons and exciton polaritons.

ACKNOWLEDGMENT

Yu. E. Lozovik was supported by RFBR Grants No. 14-02-01059 and No. 16-52-00181.

[1] J. M. Blatt, K. W. Boer, and W. Brandt, Bose-Einstein condensation of excitons, Phys. Rev. **126**, 1691 (1962).

[2] S. A. Moskalenko and D. W. Snoke, *Bose-Einstein Condensation of Excitons and Biexcitons and Coherent Nonlinear Optics with Excitons* (Cambridge University Press, Cambridge, UK, 2000).

[3] D. N. Sobyanin, Bose-einstein condensation of light: general theory, Phys. Rev. E **88**, 022132 (2013).

[4] J. Klaers, J. Schmitt, F. Vewinger, and M. Weitz, Bose-Einstein condensation of photons in an optical microcavity, Nature (London) **468**, 545 (2010).

[5] L. V. Butov, A. C. Gossard, and D. S. Chemla, Macroscopically ordered state in an exciton system, Nature (London) **418**, 751 (2002).

[6] L. V. Butov, C. W. Lai, A. L. Ivanov, A. C. Gossard, and D. S. Chemla, Towards Bose-Einstein condensation of excitons in potential traps, Nature (London) **417**, 47 (2002).

[7] R. Balili, V. Hartwell, D. Snoke, L. Pfeiffer, and K. West, Bose-Einstein condensation of microcavity polaritons in a trap, Science **316**, 1007 (2007).

[8] Yu. E. Lozovik and A. G. Semenov, Theory of superfluidity in a polariton system, Theor. Math. Phys. **154**, 319 (2008).

[9] A. Kavokin and G. Malpuech, *Thin Films and Nanostructures. Cavity Polaritons* (Elsevier Academic Press, Amsterdam, 2003).

[10] A. A. Elistratov and Yu. E. Lozovik, Coupled exciton-photon Bose condensate in path integral formalism, Phys. Rev. B **93**, 104530 (2016).

[11] M. O. Borgh, J. Keeling, and N. G. Berloff, Spatial pattern formation and polarization dynamics of a nonequilibrium spinor polariton condensate, Phys. Rev. B **81**, 235302 (2010).

[12] J. Keeling and N. G. Berloff, Spontaneous Rotating Vortex Lattices in a Pumped Decaying Condensate, Phys. Rev. Lett. **100**, 250401 (2008).

[13] J. Keeling and N. G. Berloff, Controllable half-vortex lattices in an incoherently pumped polariton condensate, arXiv:1102.5302v2.

[14] J. Kasprzak *et al.*, Bose-Einstein condensation of exciton polaritons, Nature (London) **443**, 409 (2006).

[15] P. R. Eastham and P. B. Littlewood, Bose condensation of cavity polaritons beyond the linear regime: The thermal equilibrium of a model microcavity, Phys. Rev. B **64**, 235101 (2001).

[16] V. Savona, *The Physics of Semiconductor Microcavities: From Fundamentals to Nanoscale Devices*, edited by Benoid Deveaud (Wiley-VCH, Weinheim, 2007).

[17] L. Pitaevsky and S. Stringari, *Bose-Einstein Condensation* (Clarendon, Oxford, 2003).

[18] H. Cao, Y. Y. Yamamoto, and F. Tassone, *Semiconductor Cavity Quantum Electrodynamics* (Springer, Berlin, 2000).

[19] A. Imamoglu and R. G. Ram, Quantum dynamics of exciton lasers, Phys. Lett. A **214**, 193 (1996).

[20] I. Loutsenko and D. Roubtsov, Critical Velocities in Exciton Superfluidity, Phys. Rev. Lett. **78**, 3011 (1997).

[21] L. V. Butov, A. Zrenner, G. Abstreiter, G. Bohm, and G. Weimann, Condensation of Indirect Excitons in Coupled AlAs/GaAs Quantum Wells, Phys. Rev. Lett. **73**, 304 (1994).

[22] A. V. Gorbunov and V. B. Timofeev, Large-scale coherence of the Bose condensate of spatially indirect excitons, JETP Lett. **84**, 329 (2006).

[23] D. W. Snoke, J. P. Wolfe, and A. Mysyrowicz, Evidence for Bose-Einstein condensation of excitons in Cu_2O, Phys. Rev. B **41**, 11171 (1990).

[24] V. O. Nesterenko, A. N. Novikov, A. Yu. Cherny, F. F. de Souza Cruz, and E. Suraud, An adiabatic transport of Bose-Einstein condensates in double-well traps, J. Phys. B **42**, 235303 (2009).

[25] D. Snoke, S. Denev, Y. Liu, L. Pfeiffer, and K. West, Long-range transport in excitonic dark states in coupled quantum wells, Nature (London) **418**, 754 (2002).

[26] E. Wertz, A. Amo, D. D. Solnyshkov, L. Ferrier, T. C. H. Liew, D. Sanvitto, P. Senellart, I. Sagnes, A. Lemaitre, A. V. Kavokin, G. Malpuech, and J. Bloch, Propagation and Amplification Dynamics of 1D Polariton Condensates, Phys. Rev. Lett. **109**, 216404 (2012).

[27] E. Wertz, L. Ferrier, D. D. Solnyshkov, R. Johne, D. Sanvitto, A. Lemaitre, I. Sagnes, R. Grousson, A. V. Kavokin, P. Senellart, G. Malpuech, and J. Bloch, Spontaneous formation and optical manipulation of extended polariton condensates, Nat. Phys. **6**, 860 (2010).

[28] Yu. E. Lozovik and V. I. Yudson, Feasibility of superfluidity of paired spatially separated electrons and holes; a new superconductivity mechanism, JETP Lett. **22**, 274 (1975).

[29] A. Amo, S. Pigeon, D. Sanvitto, V. G. Sala, R. Hivet, I. Carusotto, and C. Ciuti, Polariton superfluids reveal quantum hydrodynamic solitons, Science **332**, 1167 (2011).

[30] C. Anton, T. C. H. Liew, D. Sarkar, M. D. Martin, Z. Hatzopoulos, P. S. Eldridge, P. G. Savvidis, and L. Vina, Operation speed of polariton condensate switches gated by excitons, Phys. Rev. B **89**, 235312 (2014).

[31] O. L. Berman, R. Ya. Kezerashvili, and G. V. Kolmakov, Polariton-based optical switch, arXiv:1408.0304.

[32] M. De Giorgi, D. Ballarini, E. Cancellieri, F. M. Marchetti, M. H. Szymanska, C. Tejedor, R. Cingolani, E. Giacobino, A. Bramati, G. Gigli, and D. Sanvitto, Control and Ultrafast Dynamics of a Two-Fluid Polariton Switch, Phys. Rev. Lett. **109**, 266407 (2012).

[33] G. Franchetti, N. G. Berloff, and J. J. Baumberg, Exploiting quantum coherence of polaritons for ultra sensitive detectors, arXiv:1210.1187.

[34] A. Görlitz, J. M. Vogels, A. E. Leanhardt, C. Raman, T. L. Gustavson, J. R. Abo-Shaeer, A. P. Chikkatur, S. Gupta, S. Inouye, T. Rosenband, and W. Ketterle, Realization of Bose-Einstein Condensates in Lower Dimensions, Phys. Rev. Lett. **87**, 130402 (2001).

[35] A. L. Gaunt, T. F. Schmidutz, I. Gotlibovych, R. P. Smith, and Z. Hadzibabic, Bose-Einstein Condensation of Atoms in a Uniform Potential, Phys. Rev. Lett. **110**, 200406 (2013).

[36] Yu. E. Lozovik and V. I. Yudson, On the ground state of the two-dimensional non-ideal bose gas, Physica A **93**, 493 (1978).

[37] M. Schick, Two-dimensional system of hard-core bosons, Phys. Rev. A **3**, 1067 (1971).

[38] G. E. Astrakharchik, J. Boronat, I. L. Kurbakov, Yu. E. Lozovik, and F. Mazzanti, Low-dimensional weakly interacting Bose gases: Nonuniversal equations of state, Phys. Rev. A **81**, 013612 (2010).

[39] R. Desbuquois, L. Chomaz, T. Yefsah, J. Leonard, J. Beugnon, C. Weitenberg, and J. Dalibard, Superfluid behavior of two-dimensional Bose-gas, Nat. Phys. **8**, 645 (2012).

[40] F. S. Cataliotti, L. Fallani, F. Ferlaino, C. Fort, P. Maddaloni, and M. Inguscio, Superfluid current disruption in a chain of weakly coupled Bose-Einstein condensates, New J. Phys. **5**, 71 (2003).

[41] O. L. Berman, Y. E. Lozovik, and D. W. Snoke, Theory of Bose-Einstein condensation and superfluidity of two-dimensional polaritons in an in-plane harmonic potential, Phys. Rev. B **77**, 155317 (2008).